

Antimicrobial activity of GN peptides and their mode of action

Mojsoska, Biljana; Nielsen, Hanne Mørck; Jenssen, Håvard

Published in:
Biopolymers

DOI:
[10.1002/bip.22796](https://doi.org/10.1002/bip.22796)

Publication date:
2016

Document Version
Peer reviewed version

Citation for published version (APA):

Mojsoska, B., Nielsen, H. M., & Jenssen, H. (2016). Antimicrobial activity of GN peptides and their mode of action. *Biopolymers*, 106(2), 172-183. <https://doi.org/10.1002/bip.22796>

General rights

Copyright and moral rights for the publications made accessible in the public portal are retained by the authors and/or other copyright owners and it is a condition of accessing publications that users recognise and abide by the legal requirements associated with these rights.

- Users may download and print one copy of any publication from the public portal for the purpose of private study or research.
- You may not further distribute the material or use it for any profit-making activity or commercial gain.
- You may freely distribute the URL identifying the publication in the public portal.

Take down policy

If you believe that this document breaches copyright please contact rucforsk@ruc.dk providing details, and we will remove access to the work immediately and investigate your claim.

1 Antimicrobial activity of GN peptides and 2 their mode of action

3 Troels Godballe¹, Biljana Mojsoska¹, Hanne M. Nielsen², Håvard Jenssen^{1,*}

4 ¹*Dept. of Science, Systems & Models, Roskilde University, Universitetsvej 1, DK-4000 Roskilde,*
5 *Denmark.*

6 ²*Dept. of Pharmacy, Biologics, University of Copenhagen, Universitetsparken 2, 2100 Copenhagen,*
7 *Denmark.*

8 *Corresponding Author: jenssen@ruc.dk Tel +45 4674 2877

9

10 **Abstract**

11 Increasing prevalence of bacteria that carries resistance towards conventional antibiotics has prompted
12 the investigation into new compounds for bacterial intervention to ensure efficient infection control in
13 the future. One group of potential lead structures for antibiotics is antimicrobial peptides due to their
14 characteristics as naturally derived compounds with antimicrobial activity. In this study we aimed at
15 characterizing the mechanism of action of a small set of *in silico* optimized peptides. Following
16 determination of peptide activity against *E. coli*, *S. aureus* and *P. aeruginosa*, toxicity was assessed
17 revealing meaningful selectivity indexes for the majority of the peptides. Investigation of the peptides
18 effect on bacteria demonstrated a rapid growth inhibition with signs of bacterial lysis together with
19 increased bacterial size. Both visual and quantitative assays clearly demonstrated bacterial membrane
20 disruption after 10 minutes for the most active peptides. The membrane disrupting effect was verified
21 by measuring the release of calcein from bacterial mimicking liposomes. This revealed the most active
22 peptides as inducers of immediate release, indicating the kinetics of membrane permeabilization as an
23 important determinant of bacterial activity. No well-defined secondary structure of the peptides could
24 be determined using CD-spectroscopy in the presence of different liposomes mixtures, implying that
25 there is no correlation between peptide secondary structure and the observed anti-bacterial and
26 cytotoxic activity for this set of peptides. In conjunction, these findings provide strong indications of
27 membrane disruption as the primary mechanism of bacterial growth inhibition for the tested peptides.

28

29 **Keywords:** Antibacterial host defence peptides; Membrane destabilization, Antibacterial mode of
30 action; Anti-infective; b

31

32 Introduction

33 For a long time, the treatment of most infections in western countries has been considered a rather
34 uncomplicated matter due to the effectiveness of various antibiotics. Fortunately that still applies,
35 although the treatment of some bacterial infections has become gradually more complicated in recent
36 years because of the increase in bacterial resistance against conventional antibiotics. This is made
37 obvious by the fact that infectious diseases are the third leading cause of death in developed countries,
38 despite the abundant availability of antibiotics ¹.

39 The emergence of bacteria with resistance towards conventional antibiotics is increasing at an alarming
40 rate especially in hospital settings, seriously hampering effective treatment of infections ². Methicillin-
41 resistant *Staphylococcus aureus* (MRSA) was in 2005 estimated to have caused 94 000 infections
42 leading to 19 000 deaths ³ and together with other multi drug resistant (MDR) strains of *Pseudomonas*
43 *aeruginosa* and extended-spectrum-beta-lactamase (ESBL) producing *Klebisella pneumonia* and
44 *Escherichia coli*, they pose an increasing threat to public health ⁴. On top of this there has only been
45 introduced a very limited number of new antibacterial agents to the market since the 60's which
46 together with a rapid declining interest from medical companies into development of new antibiotics,
47 illustrates a development that calls for concern ^{2, 4}. In that perspective, it is important to pursue the
48 development of new antimicrobial agents, with a novel mode of action, to ensure that we will be able to
49 cure life-threatening infections in the future. One such group of compounds that has the potential to
50 assist in the fight against infections is antimicrobial peptides.

51 Antimicrobial peptides are a natural component of the innate immune system in a wide range of
52 organism, acting as a first line of defense against various microbes. These peptides have been isolated
53 from a great number of organisms ranging from bacteria to plants, invertebrates and vertebrates,
54 thereby demonstrating their prevalence in virtually all branches of life ⁵. In relation to their abundance
55 among different kinds of organisms, the biological effect varies from direct bacterial inhibition ⁵ to
56 immune modulating ⁶, proving their versatility as effector molecules. The variety in origin and
57 biological effect is reflected in the characteristics of antimicrobial peptides having a great deal of
58 diversity, in both primary and secondary structure, probably explaining their evolutionary success ⁷.
59 Even so, there are a number of structural similarities that apply for most antimicrobial peptides, usually

60 being relatively short, ranging from 12-50 amino acids, carrying a net positive charge of +2 to +9 and
61 having a distinct proportion of hydrophobic residues ⁸.

62 The positive charge of antimicrobial peptides is generally accepted as the main feature that mediates
63 selectivity towards bacteria by harboring sufficient electrochemical attraction towards the negatively
64 charged outer entities of bacterial cells to allow selective activity. As natural compounds with an
65 antimicrobial effect, antimicrobial peptides have drawn the attention of scientist to investigate their
66 potential as future antimicrobial agents. This has led to the identification of more than 1000
67 antimicrobial peptides ⁹, and numerous attempts to improve activity by modifying natural antimicrobial
68 peptides or the *de novo* design of antimicrobial peptides ¹⁰ including the use of unnatural amino acid
69 analogues ¹¹. Although a large number of natural and synthetic antimicrobial peptides have been
70 studied, there are still today, questions tied to the exact nature of bacterial inhibition exerted by these
71 peptides. Compiling evidence suggests that antimicrobial peptides have a plethora of effects against
72 bacteria, ranging from unspecific membrane perforation to specific inhibition of intracellular targets
73 and the bacterial inhibition exerted by some antimicrobial peptides is possibly the result of more than
74 just one isolated mechanism ⁵. Although different targets have been identified, a detailed
75 characterization of the mode of action has only been carried out on a minority of peptides. To truly take
76 advantage of antimicrobial peptides and make use of their potential as lead structures for bacterial
77 intervention, it is therefore in that perspective that the scope of this work is to elucidate the mechanism
78 of action of a set of different synthetic antimicrobial peptides. The antimicrobial peptides used in this
79 study were originally designed by Fjell and colleagues by the use of *in silico* screening ¹². The 10 most
80 active peptides from this optimization were selected for investigation in this study, all having a positive
81 charge of +4, uniform chain length of 9 amino acids and at least three tryptophan residues. To verify
82 the activity of the peptides, minimal inhibitory concentration (MIC) testing was carried out against *E.*
83 *coli*, *P. aeruginosa* and *S. aureus* reference strains and the two most active peptides were selected for
84 further studies to elucidate the mechanism of bacterial inhibition. Herein we demonstrate compelling
85 evidence for membrane perforation as the main contributor of bacterial inhibition together with
86 reversible metabolic disturbance at lower concentrations.

87

88 **Material and methods**

89 **Solid phase peptide synthesis**

90 The peptides were synthesized using solid phase Fmoc chemistry with amidation on the carboxyl end,
91 purified by reverse-phase HPLC using a C₁₈ column (Higgins Analytical Inc. 10 μm 250x10 mm) and a
92 water/acetonitrile gradient. The correct mass and purity >95% was verified using Dionex Ultimate 3000
93 RP-UHPLC (C18 Kinetex 100 x 2.1 mm, 100 Å) electrospray ionization mass spectrometry (Finnigan
94 LTQ) (**Figure S1, Table S1**).

95

96 **Minimal inhibitory concentration determination**

97 The antimicrobial efficacy of peptides was tested using a serial dilution titration, as previously
98 described¹³ on a panel of clinically relevant bacterial strains; i.e. *E. coli* (ATCC 25922), *P. aeruginosa*
99 PAO1 (ATCC 15692), *S. aureus* (ATCC 29213). Conventional antibiotics used throughout the study
100 include Ampicillin (A9518), Ciprofloxacin (17850), Tetracycline (T7660), Tobramycin (T4014) and
101 Polymyxin B (92301), all purchased from Sigma. In short, overnight cultures were grown to mid-log
102 phase before diluting to $\sim 5 \times 10^5$ CFU/mL in Mueller Hinton broth (Becton Dickinson) and 90 μL was
103 used to inoculate each well of a 96-well polypropylene plate (Cat. No. 3879, COSTAR). Then, 10 μL
104 aliquots of a 2-fold dilution series of the peptides were added and the minimal inhibitory concentration
105 (MIC) was scored as the lowest concentration that inhibited visible growth after 48 hours of incubation
106 at 37°C.

107

108 **Hemolysis assay**

109 Freshly drawn human blood with EDTA as anticoagulant was washed and centrifuged at 500 g for 5
110 minutes until the appearance of clear supernatant. A two-fold dilution series of peptides was added to
111 96-well polypropylene microtiter plates (COSTAR Cat. No.3879) in 75 μL aliquots together with 50
112 μL of 4 % final concentration of red blood cells (RBC) giving a total volume of 125 μL. The plate was
113 incubated with shaking for 1 hour at 37°C, before being centrifuged at 250 g for 5 minutes. 50 μL of
114 the supernatant was diluted 1:3 in sterile saline in a flat bottomed 96-well greiner plate before

115 measuring absorbance at 414 nm, using a multi-detection microplate reader Synergy HT. 100 % lysis
116 was defined as RBC treated with 1% Triton-X 100 and sterile saline treated RBC was added for
117 baseline adjustments. The test range was 3.1-400 µg/mL.

118

119 **MTT assay**

120 Toxicity against HeLa cells was estimated by the MTT viability assay. HeLa cells were cultured in
121 DMEM Glutamax media (32430-027, Invitrogen), media supplemented with 10% FBS and 1%
122 pen/strep using standard techniques. The cells were passaged at least 2 times before being used in the
123 assay, to ensure logarithmic growth. At 80 % confluency, cells were harvested, quantified and 10.000
124 cells/well were seeded in a 96-well microtiter plate. The cells were placed in a humidified 5% CO₂
125 atmosphere at 37°C for 24 hours. Media was aspirated and the cells were washed with PBS w/o Ca²⁺
126 and Mg²⁺. A mixture of peptide and DMEM media (100 µl) was added and the cells were incubated in
127 a humidified 5% CO₂ atmosphere at 37°C for 1 hour before wash with PBS with or without Ca²⁺ and
128 Mg²⁺. MTT (50 µg) dissolved in PBS with or without Ca²⁺ and Mg²⁺ was added and the cells were
129 incubated 90 minutes in a humidified 5% CO₂ atmosphere at 37°C. MTT solution was aspirated and
130 100 µL of DMSO was added to dissolve the formazan crystals before incubating 5 minutes at 37°C.
131 The absorbance at 540 nm was read in a multi-detection microplate reader Synergy HT. Viability
132 control was assigned to samples with only HeLa cells and DMEM media and 0 % viability was
133 assigned to samples with 1 % added Triton-X-100 instead of peptides. The assay was done 3 times with
134 duplicates and results are the mean of these. Concentrations giving a 50% reduction in metabolism
135 (IC₅₀), was calculated using equation (I) in Graphpad Prism.

$$136 \quad Y = \frac{100}{1 + 10^{((\text{Log}IC_{50} \div X) \cdot \text{HillSlope})}} \quad (\text{Eq. I})$$

137

138

139 Killing kinetics

140 Colony forming units (CFU) counts were monitored for 180 minutes, following peptide exposure at
141 concentration corresponding to 1×, 2× and 4×MIC. Overnight culture of *E. coli* ATCC 25922 was
142 diluted with fresh Mueller Hinton broth and re-grown to mid-log phase before diluting to a turbidity of
143 OD₆₀₀ 0.1 and loading 90 μL into wells of a flat bottomed 96-well Greiner plate containing 10 μL of
144 peptides solution. Growth control was assigned to wells without peptide. The content of individual
145 plates was collected and plated out in duplicate on LB agar plates. Between extractions, the microtiter
146 plate was sealed and placed at 37°C. LB agar plates were incubated for 18 hours at 30°C and colonies
147 were counted. The presented results are the mean of 3 independent experiments.

148 The effect of peptides on bacterial growth was investigated by monitoring optical density (OD)
149 following peptide exposure. Overnight culture of *E. coli* ATCC 25922 was diluted with fresh Mueller
150 Hinton broth and re-grown to mid-log phase before diluting to a turbidity of OD₆₀₀ 0.1. A microtiter
151 plate was filled with 10 μL of peptide or antibiotic solution per wells, before loading 90 μL of bacterial
152 suspension. For both peptides and antibiotics, concentrations corresponding to 1×-, 2×- and 4×MIC
153 were used. OD₆₀₀ was measured, with a multi-detection microplate reader Synergy HT at 37°C, every 8
154 minutes for 5 hours with shaking. The readings were baseline corrected against wells with only Mueller
155 Hinton broth. Comparison between a standard spectrophotometer, with a cuvette length of 1 cm, and
156 the readings obtained from the plate reader showed a difference with 5-fold lower readings from the
157 plate reader (data not shown). In order to make readings meaningful, in relation to the correlation
158 between optical density and concentration of bacterial cells, the readings from the plate reader was
159 multiplied with a factor of 5.

160 The effect on both bacterial DNA content and change in cell size after exposure with peptides was
161 monitored over 180 minutes by flow cytometry. An overnight culture of *E. coli* ATCC 25922 was
162 diluted with fresh Mueller Hinton broth and re-grown to mid-log phase before diluting to a turbidity of
163 OD₆₀₀ 0.1. A total of 90 μL of this bacterial suspension was loaded into a flat bottomed 96-well Greiner
164 plate for peptide and antibiotic samples and 100 μL for control samples. After extraction of the zero
165 sample, 10 μL of peptide solution corresponding to 1× and 4× the MIC concentration was added for a
166 total volume of 100 μL. Two wells were loaded for each treatment to ensure enough bacteria for the

167 flow cytometry analysis. Immediately after extraction the samples were put on ice and centrifuged at 10
168 000 g for 5 minutes at 4°C and resuspended in 100 µL 10 mM Tris HCl pH 7.4 before fixing with 1000
169 µL 77% ethanol. The following day, the samples were centrifuged at 10 000 g for 5 minutes before
170 gently removing the supernatant and adding 140 µL staining solution (90 µg/mL Mitramycin and 20
171 µg/mL ethidium bromide in 10 mM Tris pH 7.4, 10 mM MgCl₂). The samples were run on an A10
172 Bryte Flow Cytometer and when possible, 20 000 events were included in the analysis.

173

174 **Membrane depolarization assay**

175 The LIVE/DEAD® BacLight™ Bacterial Viability Kit (L7012, Invitrogen), was applied to peptide
176 treated *E. coli* ATCC 25922, to investigate a visual indication of the membrane permeability
177 capabilities of the peptides. Overnight culture of *E. coli* ATCC 25922 was diluted with fresh Mueller
178 Hinton broth and re-grown to mid-log phase before diluting to a turbidity of OD₆₀₀ 0.1. Then 10 µL of
179 peptide solution corresponding to a final test concentration of 1× and 4×MIC was added to a flat
180 bottomed polystyrene Greiner plate before loading 90 µL of bacteria suspension. 100 µL of bacterial
181 suspension was used as a control. Each well corresponded to one time point for each individual
182 treatment. The plate was placed at 37°C and the samples were extracted at the indicated time points and
183 immediately put on ice. The samples were then centrifuged at 10 000g for 5 minutes, and the pellet
184 resuspended in 100 µL 0.9% ice cold NaCl, to remove interfering media components. Staining solution
185 (1 µL) was added and incubated for 15 minutes in the dark, before loading to 1% agarose slips on
186 microscope slides. Staining solution was prepared by adding 5 µL of 3.3 mM Syto-9 dye in DMSO
187 (Compound A) and 5 µL of 20 mM Propidium iodide in DMSO (Compound B) to 20 µL of sterile
188 water. Samples were inspected with a Leica DM5000B microscope using a mercury lamp. A filter cube
189 with excitation filters of 436, 495 and 580 nm and emission filters of 460, 535 and 630 nm was used to
190 be able to detect both live and dead bacteria.

191 To verify the findings from microscope pictures with an assay that could characterize the membrane
192 permeability of the entire bacterial population in the samples, the Live/Dead quantification was
193 performed. The assay was essentially performed according to the manufacturer's instructions. After
194 establishing a standard curve from known ratios of isopropyl killed and live bacteria an overnight

195 culture of *E. coli* ATCC 25922 was diluted with fresh Mueller Hinton broth and re-grown to mid-log
196 phase before diluting to a turbidity of OD₆₀₀ 0.1. The bacterial solution and peptide solution was mixed
197 in a 9:1 ratio (vol/vol) in a 96-well polypropylene plate (Cat. No. 3879, COSTAR) and incubated at
198 37°C. At the indicated timepoints the content of individual wells was extracted, put on ice and then
199 pelleted at 11 000 g for 8 minutes before being resuspended in 0.9% NaCl and placed on ice again. The
200 resuspended bacterial suspension was then added to individual wells of flat bottomed 96-well
201 polystyrene plate and mixed with 100 µL staining solution before incubation in the dark for 15 minutes
202 and subsequent measurement of fluorescence on a multi-detection microplate reader Synergy HT.
203 Green fluorescence was excited at 485 nm and the emission detected at 528 nm, whereas the red
204 fluorescence was excited at 530 nm and detected at 645 nm. Percentage of living cells was obtained by
205 using equation (II) using the standard curve made from known ratios of live cells. The staining solution
206 was prepared by adding 3 µL of both compound A and B, for each 1 mL of distilled sterilized water
207 and stored in the dark.

$$208 \quad \% \text{ live cells} = \frac{\text{Green fluorescence}}{\text{Red fluorescence}} \cdot \frac{1}{0.0627} \quad (\text{Eq. II})$$

209 **Liposome preparation**

210 Large unilamellar vesicles (LUVs) was prepared by mixing POPC (1-palmitoyl-2-oleoyl-sn-glycero-3-
211 phosphocholine) and POPG (1-palmitoyl-2-oleoyl-sn-glycero-3-phosphoglycerol) and in a molar ratio
212 of 3:7 as a simple mimic of bacterial membranes and POPC:POPG:Cholesterol was mixed in a molar
213 ratio of 5:2:3 as a simple mimic of mammalian membrane. POPC (770557), POPG (770257) and
214 Cholesterol were all purchased from Avanti Lipids (Alabaster, Alabama). The lipid mixture was
215 concentrated on a rotary evaporator and washed 3 times with 99.9 % ethanol to remove residual
216 organic solvents. The lipid mixture was then dissolved in 4 mL HEPES buffer (10 mM HEPES, 150
217 mM KCl, 0.03 mM CaCl₂, 0.01 mM EDTA, pH 7.4) with 20 mM calcein (C0875, Sigma), for calcein
218 containing liposomes and 10 mM Tris pH 7.4 for empty liposomes used for CD spectroscopy, followed
219 by thorough mixing and sonication for 5 minutes to prevent aggregates. Subsequently, the lipid mixture
220 was vigorously whirled every 10 minutes over the course of 1 hour and finally left at room
221 temperature for 1 hour, to allow the lipids to anneal. LUVs were prepared by extruding the lipid

222 mixture through, two double stacked 100 nm filters, a total of 10 times using a Nitrogen powered
223 extruder. The calcein containing liposomes were loaded on Sephadex G-50 columns to separate
224 encapsulated calcein from free calcein and eluted with HEPES buffer. The size of the liposomes was
225 verified to be approximately 110 nm with a narrow size distribution by dynamic light scattering (DLS)
226 using a Zetasizer Nano ZS (Malvern, Worcestershire, UK). Malvern DTS v. 5.10 software (Malvern,
227 Worcestershire, UK) was used for acquisition and analysis. By comparing the end volume with the
228 starting volume, the dilution of the initial liposome concentration was estimated and that lead to the
229 anticipation of a stock concentration of 971 μM of the liposomes.

230

231 **Calcein release assay**

232 Calcein release was done in a 96-well plate with shielded wells (MicroWell 96 optical bottom plate,
233 NUNC, Roskilde, DK). 100 μL of peptide diluted in 10 mM HEPES buffer was added and immediately
234 before measurement of leakage, 80 μL of 45 μM liposome suspension was added for a final liposome
235 concentration of 20 μM . The liposome concentration was calculated from the starting concentrations of
236 lipids, taking into account the change in volume during preparation, and assuming a 100% yield from
237 the sephadex column. Measurements were performed in a FLUOstar OPTIMA plate reader at an
238 excitation wavelength of 485 nm and an emission wavelength of 520 nm over the course of 1 hour at
239 37°C. Maximum leakage of liposomes was acquired by lysis with 10% Triton and release following
240 peptide exposure, was calculated using equation (III), where F_{max} denotes fluorescence after addition of
241 10% Triton, F_0 represents background fluorescence of liposomes and F designates the fluorescence
242 intensity after peptide addition.

$$243 \quad \% \textit{leakage} = 100 \bullet \left(\frac{F - F_0}{F_{\text{max}} - F_0} \right) \quad (\text{Eq. III})$$

244

245 Results

246 This study aimed at characterizing the bacterial inhibition and antibacterial mode of action of a set of
247 highly active antimicrobial peptides earlier identified by Fjell *et al.*¹². The GN peptide library was
248 screened for antibacterial activity against Gram-negative *E. coli* ATCC 25922 and *P. aeruginosa*
249 ATCC PAO1 and Gram-positive *S. aureus* ATCC 29213 bacteria. The minimal inhibitory
250 concentrations of the tested peptides demonstrated a significant spread in activity pattern from 1.5 to
251 100 µg/mL (**Table 1**). Potent broad spectrum activity against both Gram-negative and Gram-positive
252 bacteria was observed for GN-2, GN-4 and GN-6 peptides. For specific activity against *E. coli*, GN-14
253 exhibits as good antimicrobial activity as GN-2, GN-4 and GN-6 peptides. Similarly, a pronounced
254 antimicrobial activity against *S. aureus* was observed for GN-5 peptide (1.5 µg/mL), and GN-2 and
255 GN-6 peptides (3.1 µg/mL). However, in respect to a broad spectrum antimicrobial potential, peptide
256 GN-2 and GN-4 appear as best candidates.

257 In an attempt to explain the antibacterial peptide properties with classical chemical properties the
258 hydrophobic moment was measured for all the peptides. This quantitative measure of the peptides
259 amphipathicity indicates that antibacterial activity increases proportionally with the hydrophobic
260 moment (**Table 1**). In order to further characterize the antimicrobial profiles of the GN peptides, their
261 ability to selectively target bacterial- versus mammalian cells was assessed using hemolytic assay.
262 Human red blood cells were exposed to different concentrations of GN peptides and the degree of lysis
263 was evaluated. All peptides resulted in a dose dependent release of hemoglobin, and toxicity is reported
264 as the highest concentration of peptides resulting in less than 10 % lysis compared to PBS treated
265 control cells (**Table 1**). Comparing antibacterial and hemolytic potential, the peptide library clearly
266 separates into two sub-groups; GN-8, -9, -11 and -12 being hardly hemolytic with low antimicrobial
267 potential, while the remaining peptides demonstrate an overall higher antibacterial effect yet still only
268 modest hemolytic activity. Thus, for this set of peptides the tendency to lyse human red blood cells is
269 highly correlated with the ability to kill bacteria. In comparison, indolicidin, a small 13 amino acids
270 tryptophan and arginine rich antimicrobial peptide¹⁴, is used as an antibacterial reference peptide
271 indicating that most of the GN peptides have superior selectivity. To further complement the
272 assessment of the potential toxicity of the GN peptides, a MTT assay was performed on HeLa cells and
273 the inhibitory concentrations giving 50 % reduction (IC₅₀) of cellular metabolic activity were calculated

274 (**Table 1**). The results are in agreement with the hemolytic activity, thus demonstrating that the
275 peptides with the highest antimicrobial activities are the peptides exhibiting the greatest metabolic
276 inhibition in HeLa cells. Hence, peptides GN-2 and GN-4 stand out as most cytotoxic with IC_{50} values
277 of 47 and 37 $\mu\text{g/mL}$, respectively.

278 To dissect the antimicrobial activity of GN peptides with a range of different assays, GN-2 was chosen
279 as the most potent peptide with good selectivity index range of 16 to 32. Correspondingly, GN-6 which
280 structurally differs from GN-2 peptide in the presence of phenylalanine and a patch of 4 consecutive
281 tryptophan residues was also considered for characterization for the mechanism of bacterial inhibition.

282 First to differentiate between bactericidal or bacteriostatic mode of antibacterial activity, colony
283 forming unit counts were monitored for *E. coli* cultures exposed to 1 \times , 2 \times , and 4 \times MIC concentrations
284 of GN-2 and GN-6 peptide. This assay illustrated the ability of the different peptide concentrations to
285 reduce the colony forming unit counts over a period of 180 minutes. The GN-2 peptide demonstrates
286 fast antimicrobial activity indicated by a decrease of exponentially growing bacteria within the first 40
287 minutes of exposure (**Figure 1**). The inhibition proceeds for 80 minutes after which there is a
288 reestablished bacterial growth observed. Similar pattern is observed for GN-6 peptide with a slightly
289 delayed inhibition. Bacterial inhibition is concentration dependent for both peptides, even though the
290 standard error bars for GN-6 peptide at 4 \times MIC show high experimental variation.

291 To further elucidate the bacterial inhibition exploited by the peptides, bacterial mass was monitored by
292 optical density readings at 600 nm over a course of 5 hours. The control bacteria display exponential
293 growth until 120 minutes after which clear decrease in optical density is observed. There is a
294 reestablished growth after 180 minutes, indicating that the decrease after 2 hours is not due to limited
295 nutrition and/or waste build-up (**Figure 2**). A number of antibiotics were analyzed in parallel for
296 growth inhibition patterns so that the potential bacterial targets of GN-2 and GN-6 peptides could be
297 elucidated. In addition to the viability experiments of exponentially growing *E. coli*, the optical density
298 measurements revealed clear concentration dependent inhibition of the optical density readings when
299 bacteria were exposed to 1 \times MIC concentration of both GN-2 and GN-6 peptide when compared to the
300 untreated bacteria. The inhibition is most pronounced at 2 \times MIC concentration for both peptides. With
301 respect to 1 \times MIC concentration of both peptides, the inhibition pattern is different indicating distinct

302 ways of exerting antimicrobial activity halting bacterial growth. Both peptides at 2×MIC concentration
303 demonstrate low OD measurements indicative of some degree of bacterial lysis.

304 Flow cytometry analyses were used to characterize the effect of GN-2 and GN-6 peptide on cell size
305 and DNA content. Exponentially growing *E. coli* were exposed to 1× and 4×MIC concentrations of
306 GN-2 and GN-6 peptides and samples were analyzed every 20 minutes over a course of 3 hours for
307 DNA content per cell mass extrapolated by fluorescence/lightscatter measurements. Untreated *E. coli*
308 show fairly constant ratio of DNA per cell size indicative for a healthy growing bacterial population.
309 Exposure to 1× and 4×MIC concentration of GN-2 gives pronounced initial decrease of DNA content
310 per cell size as compared with the control samples. After 40 minutes of exposure an increase of DNA
311 per cell size is observed for samples treated with 4×MIC concentration, referring to the reestablishing
312 of the DNA content at this point. At 120 minutes the effect of DNA content per cell size follows similar
313 ratio to that of the control, indicating a possible recovery (**Figure 3A**). Similar fashion of initial fast
314 and persistent decrease of DNA per cell size followed by an increase after 40 minutes is observed for
315 bacteria treated with 1×MIC concentration of GN-6 peptide.

316 The increase in cell size indicated by the lightscatter measurements observed in the flow cytometry
317 data (**Figure S2**) is supported by the microscopy images taken at time zero and 180 minutes for the
318 control *E. coli* population. Bacteria treated with GN-2 peptide at 1× and 4×MIC concentration appear
319 slightly bigger in size than the control bacteria. Clear difference between cells treated with 1× and
320 4×MIC concentrations of GN-2 peptide is observed by the large areas of cell debris and bacteria
321 transparency indicating cell lysis in samples treated with 4×MIC (**Figure 3C**). Upon treatment with
322 GN-6 peptide at 4×MIC concentrations, there is a clear morphological change presented by cells that
323 appear long and filamentous but not lysed (**Figure 3C**). This data is in agreement with the observations
324 from the flow cytometry analyzes on DNA, size and DNA /size.

325 Live/dead staining experiments with SYTO9 green-fluorescent nucleic acid stain and propidium iodide
326 red-fluorescent stain, were used to analyze the membrane permeability capacity of GN-2. Under
327 conditions where no membrane permeabilizing agent is present, bacteria with intact membranes will
328 stain green (**Figure 4A**). The un-treated control cells are naturally predominantly staining green at all
329 time-points, illustrating a healthy population of bacteria. *E. coli* exposed to GN-2 peptide at 1×MIC

330 concentration at the 10 and 20 minutes time-point, demonstrate about 90 % permeabilized membranes,
331 thus staining red. However, over time the surviving cells are replicating, resulting in an increasing
332 percentage of green cells in the later time points (**Figure 4B**). Upon increasing the GN-2 peptide
333 concentration to 4×MIC, the membrane integrity stays disrupted throughout the assay of 120 minutes
334 (**Figure 4C**). To quantify the membrane permeability in a more un-biased fashion than microscopy, the
335 same bacterial cultures were also analyzed using a multi-detection fluorescence plate reader. Plotting
336 the ratio of live and dead cells for cultures incubated with 1×, 2× and 4×MIC concentration of GN-2
337 peptide over time, clearly demonstrates how 2× and 4×MIC knocks down the viability to around 20%
338 and this level is kept for 120 minutes. Contrary, at 1×MIC of GN-2, the level of viable bacteria after 10
339 minutes is about the same as in the samples treated with 2× and 4×MIC of GN-2, but at 1×MIC the
340 culture re-grows with a doubling time of about 1 hour (**Figure 4D**).

341 Due to previously established observation of membrane disruption as a primary mode of action of the
342 GN peptides, calcein leakage assay was performed. This assay allows characterization of peptides
343 based on the different potencies to provoke membrane leakage of calcein entrapped unilamellar
344 phospholipid vesicles (LUVs) made of POPC:POPG (3:7 molar ratio). Calcein is a self-quenching
345 molecule that at high concentration shows relatively low background fluorescence. As calcein
346 molecules are being released to the exterior of the vesicles, the fluorescence increases. The percentage
347 of calcein leakage can be plotted as a function of the concentration of the peptides. All GN peptides
348 were able to induce calcein leakage in a concentration dependent manner at endpoint reading of 60 min
349 (**Figure 5A**). But the release of calcein is much less significant that what is induced by melittin, a well-
350 known peptide with non-selective lytic properties, used as a positive control for giving distinct pattern
351 of liposome disruption ¹⁵.

352 As it was impossible to distinguish the lytic potential of the different GN peptides using an endpoint
353 reading the release of calcein over time was monitored, enabling us to extract information about the
354 capability of the peptides to induce calcein leakage. The GN-2 peptide demonstrates distinct kinetics of
355 rapidly provoking calcein release from the liposomes, particularly at high concentrations (**Figure 5B**).
356 Only a small concentration change from 3.5 µg/mL to 5.5 µg/mL of GN-2, changes the calcein release
357 from about 30% to 100%. Conversely, the GN-6 peptide, which has slightly lower antimicrobial
358 activity than GN-2, exerts a much more gradual release of calcein over time, which stabilizes after

359 about 10 minutes (**Figure 5C**). The gradual release is observed for a wider range of concentrations,
360 suggesting different mode of membrane activity or different modes of action for this peptide compared
361 to GN-2. This could potentially be reconfirmed and better characterized using the experimental design
362 of Russel *et al.* 2010¹⁶. A similar, but even more dramatic profile for gradual release is observed for
363 GN-14 where gradual increase in calcein leakage progressing over a course of 20 minutes is observed
364 (**Figure 5D**). The different patterns of calcein leakage attribute to the correlation of antimicrobial
365 peptide activity and their ability to disrupt bacterial membranes, where more active peptides cause
366 more instantaneous release of calcein from the liposome.

367 The secondary structure of GN peptides and melittin was inspected with circular dichroism (CD)
368 spectroscopy to see whether or not a confined structure is necessary for the antimicrobial, toxic or
369 membrane disrupting activities observed. Peptide secondary structures were measured in Tris buffer pH
370 7.4 and unilamellar phospholipid vesicles consisting of POPC:POPG:Cholesterol (5:2:3 molar ratio)
371 and POPC:POPG (3:7 molar ratio), the latter mimicking mammalian and bacterial membranes,
372 respectively (**Figure S3**). None of the peptides demonstrated any defined secondary structures in Tris
373 buffer, indicating random coils under these conditions. In presence of LUV that mimic mammalian
374 membranes, the control peptide melittin adopts a structural confirmation similar to that of an α -helix
375 with peak minima at 222 and 208 nm¹⁷. Using the DichroWeb K2D algorithm¹⁸, the α -helix content in
376 melittin was calculated to be 77 % which is in agreement with other publications¹⁹. The CD spectra for
377 the GN peptides are similar for mammalian and bacterial membrane mimics and illustrate no well-
378 defined secondary structure in either environment. Therefore, it is reasonable to assume that GN
379 peptides exert their antimicrobial, toxic and membrane disrupting activity without adapting any well-
380 defined secondary structure.

381

382

383 Discussion

384 Due to the increased number of infectious agents that are resistant to many well-known classes of
385 antibiotics, there is a constant need of improved alternative drug classes and therapies. In this study we
386 present evaluation of the antimicrobial potencies of ten different peptides, GN-2 to GN-14, from the *in*
387 *silico* optimized peptide library previously reported on by Fjell *et al.*¹². These peptides are rich in
388 tryptophan residues along with lysine and arginine in various orders along the backbone (**Table 1**). The
389 contribution of the arginine, lysine and tryptophan residues to the antimicrobial activity is exerted by
390 primary interaction of the charged residues with the net negative charge distributed on the surface of
391 the bacterial membranes followed by insertion of tryptophan residues in the interfacial region of the
392 phospholipid bilayer²⁰. Beneficial features within the GN peptide library that exhibit somewhat higher
393 antimicrobial activity than others are the cationic and bulky three residues in the amino terminal with
394 specific annotation to the cationic residues which mediate interaction with the anionic lipids and lead to
395 membrane instability in Gram-negative bacteria models²¹. This observation is further supported with
396 the GN peptides -8, -9, -11 and -14 which have either leucine or isoleucine in addition to one cationic
397 (either lysine or arginine) and one tryptophan residues within their structure and exhibit lower
398 antimicrobial activities.

399 To understand the overall activity of the GN peptides and their ability to selectively discriminate
400 between bacterial and mammalian membranes, and therefore obtain a selectivity index as a ranking tool
401 for the most potential peptide candidate, hemolytic and toxic effects were investigated. A strong
402 relationship between hydrophobicity and high antimicrobial activity and high toxicity has been reported
403 in the literature²². Such observation could not be observed in this study for the GN peptides. GN-2 and
404 GN-4 are the most active against both Gram-positive and Gram-negative bacteria and have both high
405 hemolytic profiles. They share the same charge distribution along their backbone differing only in
406 isoleucine (GN-2) and leucine (GN-4) at the C-terminal end and arginine (GN-2) and lysine (GN-4) at
407 the 4th position. The last feature suggests that the lysine residue in GN-4 peptide, which is previously
408 ascribed as a contributor to the higher lytic effects²¹, exerts the same effect when compared to arginine
409 in GN-2 peptide (**Table 1**).

410 For a better differentiation of host cell toxicity, metabolic activities in HeLa cells were also monitored.
411 Comparing toxicity against HeLa cells with the hemolytic properties of the GN peptides, reveals a
412 disproportionally high toxicity towards the former (**Table 1**). This could be related to the peptides
413 exerting higher selectivity to the more anionic cancer cells, similar to previous observations²³. In
414 addition, peptides that successfully entered HeLa cells could target intracellular membranes that
415 resemble bacterial membrane such is the mitochondrial membrane and therefore inhibit metabolism
416 that could be lethal to eukaryotic cells²⁴. To further elucidate the observed toxicity of GN-2 and GN-4,
417 peptides toxicity measurements on a non-cancerous mammalian cells or animal studies should be
418 employed.

419 The current study demonstrate a fast decrease of exponentially growing *E. coli* when exposed to sub-
420 MIC concentrations of both peptide GN-2 and GN-6 (**Figure 1 and 2**). The observed decrease is
421 probably due to metabolic disturbance that halts bacterial growth for about 80 minutes, after which the
422 growth is reestablished. This is also in agreement with the OD measurements, which revealed similar
423 decrease in the bacteria growth under the same conditions. Flow cytometry analysis show that over a
424 period of 80 minutes the cell size at MIC concentrations does not change significantly, thus supporting
425 the above stated evidence (**Figure S2**). In support of this, the microscopic images reveal no obvious
426 morphological difference except that the MIC treated samples appear slightly bigger in size. The
427 increase in cell size is a result of metabolic inhibition which delays the decrease in cell size which is
428 normally observed when bacterial suspension gets denser²⁵. In contrast to the bacteriostatic inhibition
429 at MIC concentration of both the GN-2 and GN-6 peptide, bactericidal inhibition is observed at 4×MIC
430 concentrations. Inhibition through bacterial lysis is ascribed to GN-2 peptide which causes decrease in
431 OD of *E. coli* over time, and such relationship has also been described in the literature²⁶. The
432 mechanism behind the bactericidal killing for GN-6 demonstrates no signs of lysis rather than
433 filamentation which are reported as an increase in the lightscatter from the flow cytometry analysis²⁷.
434 These results are further corroborated by the microscopy studies. Prior studies have shown that the SOS
435 response to ciprofloxacin and beta-lactams is ascribed to filamentation²⁸ and the same can be induced
436 by multiple environmental stresses²⁹.

437 Disturbed membrane integrity of *E. coli* is observed after 10-20 minutes of exposure of 1×MIC
438 concentration of GN-2 peptide, followed by gradual reestablishment or growth of cells that survived

439 the initial attack (**Figure 4**). The latter seems plausible as cells surviving exposure to the peptide would
440 be in a rough and rather hostile environment, thus explaining their very slow growth. The phenomena
441 observed between 40 and 80 minutes, does also correlates with the observations of constant cell size
442 from flow cytometry analysis and a standstill in CFU. However, using live/dead staining analysis the
443 reestablishment of membrane integrity has been ascribed to membrane reassembly which leads to
444 propidium iodide exclusion³⁰ or possible efflux pumps that drive propidium iodide out of the cell³¹.
445 The later mechanism would require presence of ATP for efflux pumps which could be in agreement
446 with membrane leakage and escape of ions upon peptides acting on membranes at low concentrations,
447 provoking ATP production³². In summary, it may seem as GN-2 induce sufficient membrane
448 permeabilization for the entry of propidium iodine, but the process does not translate into full loss of
449 viability. In relation to this observation, prior studies have shown that Bac8c, a peptide with sticking
450 resemblance to the GN peptides, can causes membrane depolarization after 5 minutes of exposure
451 followed by membrane recovery after 90 minutes³³. In case of 2× and 4×MIC concentrations of GN-2
452 peptide, the peptide consistently causes membrane leakage supported by the visual and quantitative
453 membrane leakage assays supported by CFU counts that show loss of bacterial viability (**Figure 3 and**
454 **4**).

455 The GN-2 peptide with a very narrow concentration range from 5.5 to 1.7 µg/mL induced instant
456 release of calcein from model membranes, corresponding to 100% and 5%, respectively (**Figure 5**).
457 This observation coincides with a proposed model of membrane active antimicrobial peptides binding
458 to the surface of the phospholipids parallel to the membrane (S-state) and upon reaching a threshold
459 change their orientation into perpendicular position (I-state), thereby inducing a more profound
460 membrane disruption³². The GN-14 peptide revealed a more gradual release of calcein content which
461 progresses over a period of 20 minutes. Such release has been ascribed to a mechanism of transient
462 pore formation³⁴ where liposomes re-stabilize resulting in plateau state of calcein release³⁴⁻³⁵, leaving
463 partially depleted liposomes. Given that the GN peptides only are composed of 9 amino acids, the
464 toroidal pore model is the more plausible mechanism of membrane action due to the fact that the pores
465 in this model are stabilized by both lipids and peptides rather than only peptides as in the barrel-stave
466 model³⁴. A membrane mechanism involving toroidal pores are further supported by the lack of well

467 defined secondary structures in the GN peptide library (**Figure S3**), and none helical peptides have also
468 by others been demonstrated to work through this mechanism ³⁶.

469 Previous studies have shown that melittin is a pore forming membrane active peptide that acts in an all
470 or none manner ^{19c,37}, resulting in these immediate release profiles of calcein. Since the current study
471 showed similar kinetics in mediating calcein release for both melittin and GN-2, it is reasonable to
472 assume that the GN-2 peptide also acts by pore formation mechanism. However the calcein release for
473 melittin is much more pronounced at lower concentrations when compared to the release for peptide
474 GN-2 Fig.5A. Having said that it is important to stress out that melittin and GN-2 act with different
475 potencies of 16.3 (3.5 µg/mL) lipid/peptide molar ratio for melittin and 5.4 (5.5 µg/mL) for the GN-2
476 peptide. Furthermore, we would argue that GN-6 which results in a much more gradual release of
477 calcein, also could work through pore formation. The difference in kinetics of these peptides (GN-2
478 and GN-6) might be related to the lifetime of the pores ^{35,38}, the size of the pores and the number of
479 pores ³⁸, all of which reflects on the release of the entrapped molecules from the LUVs. Even though
480 pore formation may seem the best mechanism of action of tested GN peptides, the possibility of
481 membrane disruption exploited by a mixture of different mechanism should not be excluded ³⁹. The
482 release of calcein for both peptides, GN-2 and GN-6, levels off over time (Figure 5B-C) and this type
483 of behavior has been reported to indicate transient pore formation during the initial insertion step into
484 the lipid bilayer ³⁴.

485 In conclusion, based on the experimental data obtained in the current study the primary antibacterial
486 mechanism of action of GN-2 and GN-6 is associated with membrane permeabilization at high peptide
487 concentrations with different kinetics and potencies. At more moderate peptide concentrations it
488 appears that the peptides affect on metabolic disturbance, and further work is required to strengthen
489 these observations.

490

491 **Acknowledgements**

492 This work was in part funded by The Danish Council for Independent Research (grant # 10-085287).

493 We also acknowledge Professor Lars Holm Øgødal (Niels Bohr Institute, Copenhagen University) for

494 dynamic light scattering measurements of our liposomes, and Jacob Krake (Roskilde University) for
495 LC-MS analysis.

496

497 References

- 498 1. Nathan, C., Antibiotics at the crossroads. *Nature* **2004**, *431* (7011), 899-902.
- 499 2. von Nussbaum, F.; Brands, M.; Hinzen, B.; Weigand, S.; Habich, D., Antibacterial natural products in
500 medicinal chemistry--exodus or revival? *Angew Chem Int Ed Engl* **2006**, *45* (31), 5072-129.
- 501 3. Klevens, R. M.; Morrison, M. A.; Nadle, J.; Petit, S.; Gershman, K.; Ray, S.; Harrison, L. H.; Lynfield, R.;
502 Dumyati, G.; Townes, J. M.; Craig, A. S.; Zell, E. R.; Fosheim, G. E.; McDougal, L. K.; Carey, R. B.; Fridkin, S. K.,
503 Invasive methicillin-resistant *Staphylococcus aureus* infections in the United States. *JAMA* **2007**, *298* (15),
504 1763-71.
- 505 4. Fischbach, M. A.; Walsh, C. T., Antibiotics for emerging pathogens. *Science* **2009**, *325* (5944), 1089-93.
- 506 5. Jenssen, H.; Hamill, P.; Hancock, R. E., Peptide antimicrobial agents. *Clin Microbiol Rev* **2006**, *19* (3), 491-
507 511.
- 508 6. Hamill, P.; Brown, K.; Jenssen, H.; Hancock, R. E., Novel anti-infectives: is host defence the answer? *Curr*
509 *Opin Biotechnol* **2008**, *19* (6), 628-36.
- 510 7. Hale, J. D.; Hancock, R. E., Alternative mechanisms of action of cationic antimicrobial peptides on bacteria.
511 *Expert Rev Anti Infect Ther* **2007**, *5* (6), 951-9.
- 512 8. Jenssen, H.; Hancock, R. E., Antimicrobial properties of lactoferrin. *Biochimie* **2009**, *91* (1), 19-29.
- 513 9. Wang, G.; Li, X.; Wang, Z., APD2: the updated antimicrobial peptide database and its application in peptide
514 design. *Nucleic Acids Res* **2009**, *37* (Database issue), D933-7.
- 515 10. Fjell, C. D.; Jenssen, H.; Hilpert, K.; Cheung, W. A.; Pante, N.; Hancock, R. E.; Cherkasov, A., Identification of
516 novel antibacterial peptides by chemoinformatics and machine learning. *J Med Chem* **2009**, *52* (7), 2006-15.
- 517 11. Godballe, T.; Nilsson, L. L.; Petersen, P. D.; Jenssen, H., Antimicrobial beta-peptides and alpha-peptoids.
518 *Chem Biol Drug Des* **2011**, *77* (2), 107-16.
- 519 12. Fjell, C. D.; Jenssen, H.; Cheung, W. A.; Hancock, R. E.; Cherkasov, A., Optimization of antibacterial peptides
520 by genetic algorithms and cheminformatics. *Chem Biol Drug Des* **2011**, *77* (1), 48-56.
- 521 13. Wiegand, I.; Hilpert, K.; Hancock, R. E., Agar and broth dilution methods to determine the minimal
522 inhibitory concentration (MIC) of antimicrobial substances. *Nat Protoc* **2008**, *3* (2), 163-75.
- 523 14. (a) Falla, T. J.; Karunaratne, D. N.; Hancock, R. E. W., Mode of action of the antimicrobial peptide
524 indolicidin. *Journal of Biological Chemistry* **1996**, *271* (32), 19298-19303; (b) Selsted, M. E.; Novotny, M. J.;
525 Morris, W. L.; Tang, Y. Q.; Smith, W.; Cullor, J. S., Indolicidin, a novel bactericidal tridecapeptide amide from
526 neutrophils. *The Journal of biological chemistry* **1992**, *267* (7), 4292-5.
- 527 15. Shai, Y., Mode of action of membrane active antimicrobial peptides. *Biopolymers* **2002**, *66* (4), 236-48.
- 528 16. Russell, A. L.; Kennedy, A. M.; Spuches, A. M.; Venugopal, D.; Bhonsle, J. B.; Hicks, R. P., Spectroscopic and
529 thermodynamic evidence for antimicrobial peptide membrane selectivity. *Chem Phys Lipids* **2010**, *163* (6),
530 488-97.
- 531 17. Greenfield, N. J., Using circular dichroism spectra to estimate protein secondary structure. *Nat Protoc* **2006**,
532 *1* (6), 2876-90.
- 533 18. Whitmore, L.; Wallace, B. A., Protein secondary structure analyses from circular dichroism spectroscopy:
534 methods and reference databases. *Biopolymers* **2008**, *89* (5), 392-400.

- 535 19. (a) Bechinger, B., Structure and functions of channel-forming peptides: magainins, cecropins, melittin and
536 alamethicin. *The Journal of membrane biology* **1997**, *156* (3), 197-211; (b) Brogden, K. A., Antimicrobial
537 peptides: pore formers or metabolic inhibitors in bacteria? *Nature reviews. Microbiology* **2005**, *3* (3), 238-
538 50; (c) Wessman, P.; Stromstedt, A. A.; Malmsten, M.; Edwards, K., Melittin-lipid bilayer interactions and
539 the role of cholesterol. *Biophysical journal* **2008**, *95* (9), 4324-36.
- 540 20. (a) Chan, D. I.; Prenner, E. J.; Vogel, H. J., Tryptophan- and arginine-rich antimicrobial peptides: structures
541 and mechanisms of action. *Biochimica et biophysica acta* **2006**, *1758* (9), 1184-202; (b) Schibli, D. J.; Epand,
542 R. F.; Vogel, H. J.; Epand, R. M., Tryptophan-rich antimicrobial peptides: comparative properties and
543 membrane interactions. *Biochem Cell Biol* **2002**, *80* (5), 667-77.
- 544 21. Wadhvani, P.; Epand, R. F.; Heidenreich, N.; Burck, J.; Ulrich, A. S.; Epand, R. M., Membrane-active
545 peptides and the clustering of anionic lipids. *Biophysical journal* **2012**, *103* (2), 265-74.
- 546 22. Chen, Y.; Guarnieri, M. T.; Vasil, A. I.; Vasil, M. L.; Mant, C. T.; Hodges, R. S., Role of peptide hydrophobicity
547 in the mechanism of action of alpha-helical antimicrobial peptides. *Antimicrobial agents and chemotherapy*
548 **2007**, *51* (4), 1398-406.
- 549 23. Slaninova, J.; Mlsova, V.; Kroupova, H.; Alan, L.; Tumova, T.; Monincova, L.; Borovickova, L.; Fucik, V.;
550 Cerovsky, V., Toxicity study of antimicrobial peptides from wild bee venom and their analogs toward
551 mammalian normal and cancer cells. *Peptides* **2012**, *33* (1), 18-26.
- 552 24. Eliassen, L. T.; Berge, G.; Leknessund, A.; Wikman, M.; Lindin, I.; Lokke, C.; Ponthan, F.; Johnsen, J. I.;
553 Sveinbjornsson, B.; Kogner, P.; Flaegstad, T.; Rekdal, O., The antimicrobial peptide, lactoferricin B, is
554 cytotoxic to neuroblastoma cells in vitro and inhibits xenograft growth in vivo. *International journal of*
555 *cancer. Journal international du cancer* **2006**, *119* (3), 493-500.
- 556 25. Steen, H. B., Flow cytometry of bacteria: glimpses from the past with a view to the future. *J Microbiol*
557 *Methods* **2000**, *42* (1), 65-74.
- 558 26. Pasotti, L.; Zucca, S.; Lupotto, M.; Cusella De Angelis, M. G.; Magni, P., Characterization of a synthetic
559 bacterial self-destruction device for programmed cell death and for recombinant proteins release. *Journal*
560 *of biological engineering* **2011**, *5*, 8.
- 561 27. Walberg, M.; Gaustad, P.; Steen, H. B., Rapid assessment of ceftazidime, ciprofloxacin, and gentamicin
562 susceptibility in exponentially-growing *E. coli* cells by means of flow cytometry. *Cytometry* **1997**, *27* (2),
563 169-78.
- 564 28. Kohanski, M. A.; Dwyer, D. J.; Collins, J. J., How antibiotics kill bacteria: from targets to networks. *Nature*
565 *reviews. Microbiology* **2010**, *8* (6), 423-35.
- 566 29. Galhardo, R. S.; Hastings, P. J.; Rosenberg, S. M., Mutation as a stress response and the regulation of
567 evolvability. *Critical reviews in biochemistry and molecular biology* **2007**, *42* (5), 399-435.
- 568 30. Moussa, M.; Perrier-Cornet, J. M.; Gervais, P., Damage in *Escherichia coli* cells treated with a combination
569 of high hydrostatic pressure and subzero temperature. *Appl Environ Microbiol* **2007**, *73* (20), 6508-18.
- 570 31. Stocks, S. M., Mechanism and use of the commercially available viability stain, BacLight. *Cytometry A* **2004**,
571 *61* (2), 189-95.
- 572 32. Huang, H. W., Molecular mechanism of antimicrobial peptides: the origin of cooperativity. *Biochimica et*
573 *biophysica acta* **2006**, *1758* (9), 1292-302.
- 574 33. Spindler, E. C.; Hale, J. D.; Giddings, T. H., Jr.; Hancock, R. E.; Gill, R. T., Deciphering the mode of action of
575 the synthetic antimicrobial peptide Bac8c. *Antimicrobial agents and chemotherapy* **2011**, *55* (4), 1706-16.
- 576 34. Hugonin, L.; Vukojevic, V.; Bakalkin, G.; Graslund, A., Membrane leakage induced by dynorphins. *FEBS*
577 *letters* **2006**, *580* (13), 3201-5.
- 578 35. Arbuzova, A.; Schwarz, G., Pore-forming action of mastoparan peptides on liposomes: a quantitative
579 analysis. *Biochimica et biophysica acta* **1999**, *1420* (1-2), 139-52.

- 580 36. (a) Irudayam, S. J.; Berkowitz, M. L., Influence of the arrangement and secondary structure of melittin
581 peptides on the formation and stability of toroidal pores. *Biochimica et biophysica acta* 2011, 1808 (9),
582 2258-66; (b) Sengupta, D.; Leontiadou, H.; Mark, A. E.; Marrink, S. J., Toroidal pores formed by
583 antimicrobial peptides show significant disorder. *Biochim Biophys Acta* 2008, 1778 (10), 2308-17.
- 584 37. Allende, D.; Simon, S. A.; McIntosh, T. J., Melittin-induced bilayer leakage depends on lipid material
585 properties: evidence for toroidal pores. *Biophysical journal* 2005, 88 (3), 1828-37.
- 586 38. Rex, S.; Schwarz, G., Quantitative studies on the melittin-induced leakage mechanism of lipid vesicles.
587 *Biochemistry* 1998, 37 (8), 2336-45.
- 588 39. (a) Pistolesi, S.; Pogni, R.; Feix, J. B., Membrane insertion and bilayer perturbation by antimicrobial peptide
589 CM15. *Biophys J* 2007, 93 (5), 1651-60; (b) Teixeira, V.; Feio, M. J.; Bastos, M., Role of lipids in the
590 interaction of antimicrobial peptides with membranes. *Progress in lipid research* 2012, 51 (2), 149-77.
591
592

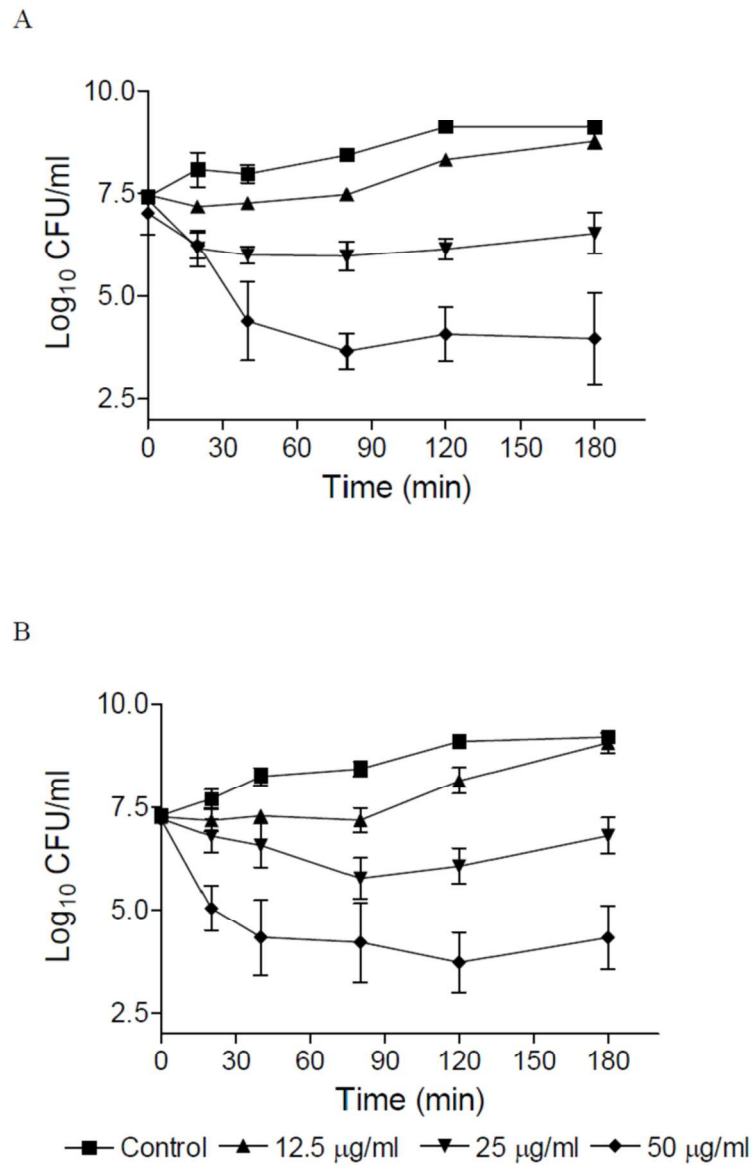


Figure 1. Viability of exponentially growing *E. coli* ATCC 25922 exposed to 1x, 2x, and 4x MIC concentrations of (A) GN-2 peptide and (B) GN-6 peptide over a course of 3 hours. Data represent mean and SEM of 3 independent experiments.
97x148mm (600 x 600 DPI)

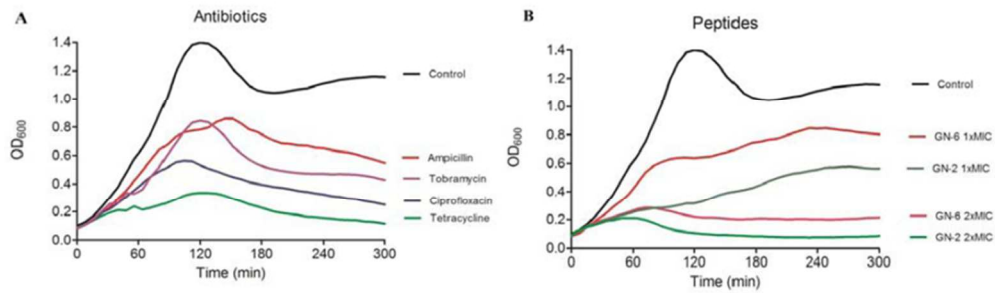


Figure 2. Optical density measurements of exponentially growing *E. coli* ATCC 25922 over 5 hours. Data presents mean of 3 independent experiments based. Bacterial growth at 37°C in a 96-well plates from a starting inoculum of OD₆₀₀ of 0.1 has been measured with 8 minutes intervals. (A) Bacteria exposed to antibiotics at MIC concentrations, Ampicillin (4 µg/ml), Tobramycin (0.78 µg/ml), Tetracycline (1 µg/ml) and Ciprofloxacin (0.05 µg/ml). (B) Bacteria exposed to GN-2 peptide at 1x MIC (6.2 µg/ml) and 2x MIC (12.5 µg/ml) and GN-6 peptide at 1x MIC (12.5 µg/ml) and 2x MIC (25 µg/ml) concentrations.
42x12mm (600 x 600 DPI)

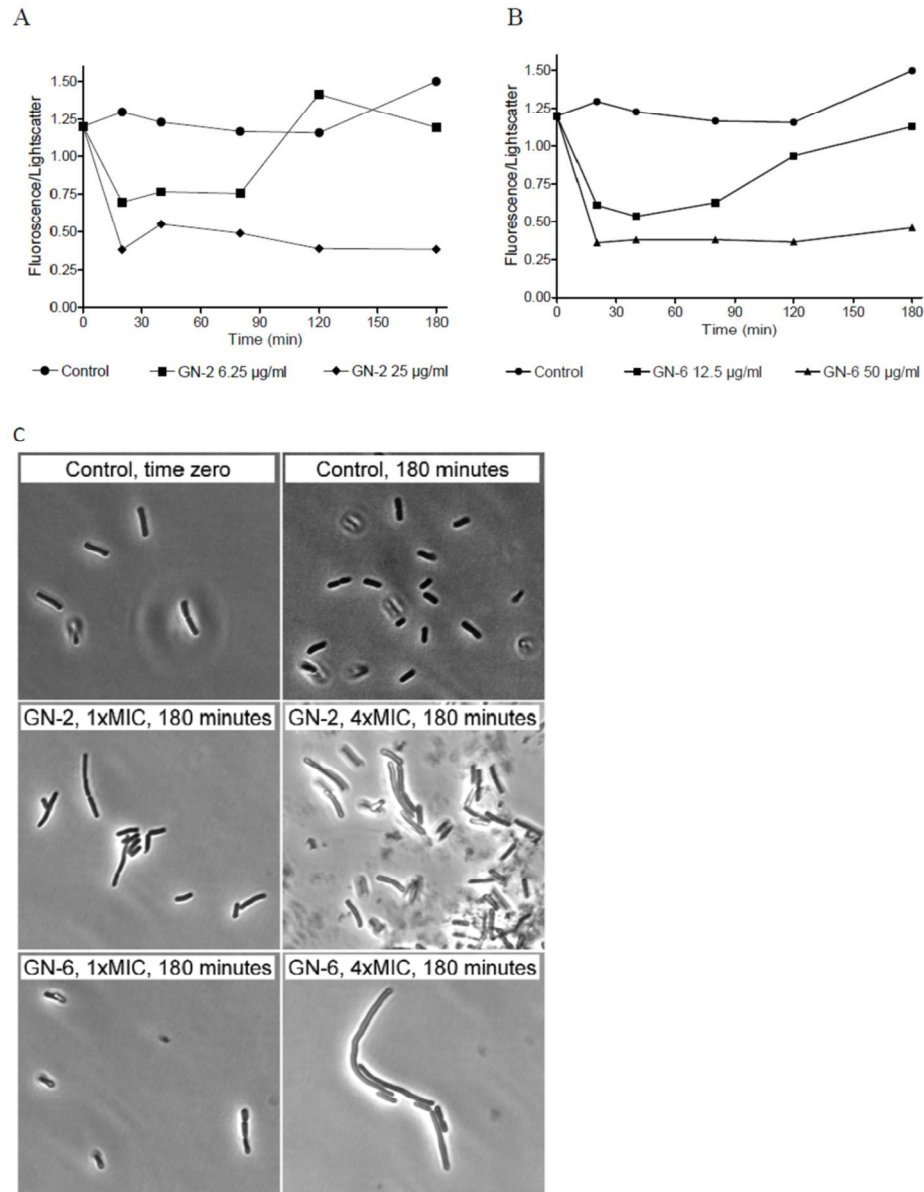


Figure 3. Peptide effect on *E. coli* morphology. (A,B) Flow cytometry data of GN-2 and GN-6 peptide influence on the DNA content per cell mass represented by fluorescence/lightscatterer ratio, respectively. Data collected over a course of 3 hours in a microtiter plate format with an inoculum of OD600 of 0.1 and incubated at 37°C between extractions. (C) Microscope images of ethanol stained flow cytometry samples of *E. coli* treated with GN-2 and GN-6 peptide at 1x and 4xMIC concentration for 3 hours. Bacteria without cellular content appear transparent. Pictures taken at same magnification with a Leica DM5000 B microscope.
87x113mm (600 x 600 DPI)

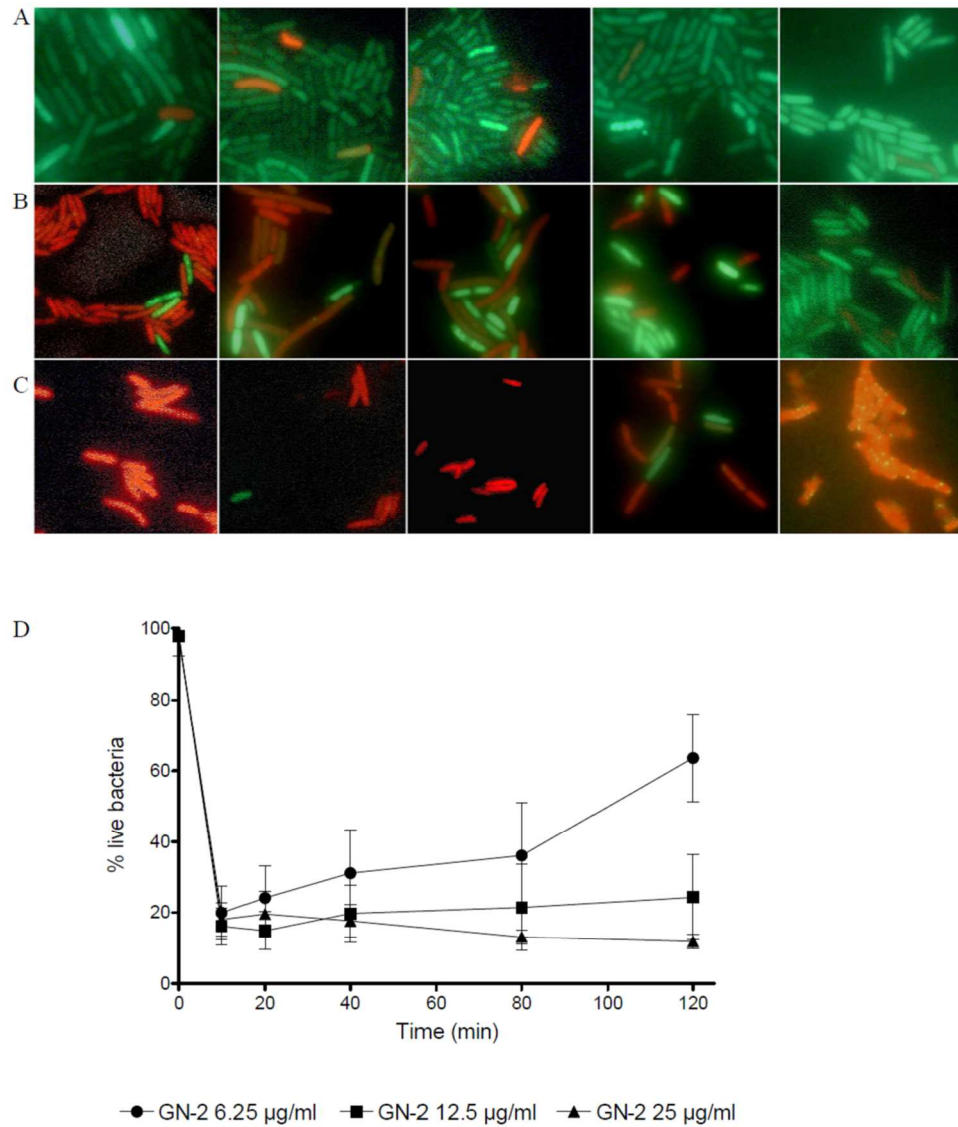


Figure 4. Visualization and quantification of membrane permeabilization of GN-2 peptide on *E. coli* ATCC 25922 over a period of 120 minutes. (A) Control cells. (B) Bacteria exposed to 1xMIC GN-2 peptide. (C) Bacteria exposed to 4xMIC GN-2 peptide. (D) Percentage of live bacteria after treatment with 1x, 2x and 4xMIC concentration of peptide GN-2. Pictures taken with Leica DM5000B microscope using mercury lamp. 118x138mm (600 x 600 DPI)

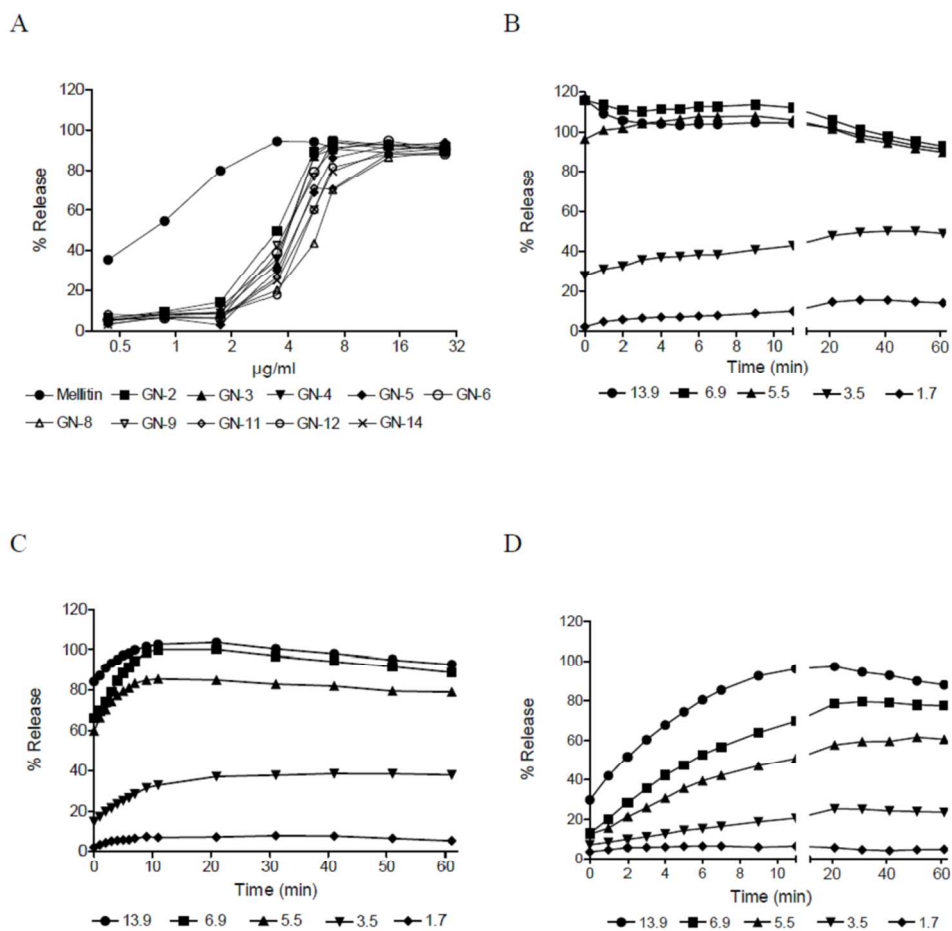


Figure 5. Calcein release from POPG:POPC vesicles. (A) Calcein leakage measurements from 20 μM POPG:POPC (7:3) vesicles at 37°C at various peptide concentrations in a 96-well format assay at 60 min. All readings are baseline corrected by subtracting values from wells containing only liposomes. 100% leakage is estimated as a total calcein release from liposomes exposed to 10 % Triton X-100. Represented results are mean values of three independent experiments with good reproducibility. Standard error bars are omitted for clarity. Calcein leakage measurements from 20 μM POPG:POPC (7:3) vesicles at 37°C at various concentrations of (B) GN-2, (C) GN-6 and (D) GN-14, in a 96-well format assay over a period of 1 hour. 76x74mm (600 x 600 DPI)

Table 1. Peptide characteristics, antimicrobial activity and toxicity

Peptide	Sequence	HPLC retention-time (min)	Hydrophobic moment	Minimal Inhibitory Concentration (µg/ml)			< 10 % Hemolysis	IC50
				<i>E. coli</i>	<i>P. aeruginosa</i>	<i>S. aureus</i>		
GN-2	RWKRWWRWI-CONH ₂	6.33	5.4	6.2	3.1	3.1	100	47
GN-3	KWWRWRRWW-CONH ₂	6.62	3.3	12.5	25	6.2	100	106
GN-4	RWKKWWRWL-CONH ₂	6.54	5.5	6.2	3.1	6.2	100	37
GN-5	KKRWWWWWR-CONH ₂	7.10	2.8	12.5	6.2	1.5	100	131
GN-6	RKRWWWWFR-CONH ₂	7.08	2.8	12.5	6.2	3.1	100	97
GN-8	IWKRWWWKR-CONH ₂	4.54	2.2	25	100	50	> 400	199
GN-9	RIWKIWWKR-CONH ₂	4.63	4.8	25	25	> 50	> 400	> 200
GN-11	IKWKRWWWR-CONH ₂	5.88	3.4	12.5	50	25	> 400	> 200
GN-12	KWWKIWRWR-CONH ₂	6.13	2.9	25	12.5	12.5	> 400	173
GN-14	RLWKRWWIR-CONH ₂	4.43	4.4	6.2	100	25	100	> 200
Indolicidin	ILPWKWPWWPWR-CONH ₂	ND	1.2	25	100	12.5	100	> 200

Table 1: Hydrophobic moment is a quantitative measure of amphipathicity calculated with HydroMCalc using the CCS scale. Median MIC values of GN peptides in µg/ml against *E. coli* ATCC 25922, *P. aeruginosa* PA01 and *S. aureus* ATCC 29213 obtained by 3 repeated experiments. Hemolysis values are the mean concentration in µg/ml recorded over 3 experiments that induced less than 10% hemolysis. IC50 values in µg/ml is a toxicity measurement resulting from the MTT assays performed on HeLa cells, and calculated from the equation $Y = \text{Bottom} + (\text{Top} - \text{Bottom}) / (1 + 10^{((\text{LogIC50} - X) * \text{HillSlope}))}$.

Figure 1. Viability of exponentially growing *E. coli* ATCC 25922 exposed to 1x, 2x, and 4x MIC concentrations of (A) GN-2 peptide and (B) GN-6 peptide over a course of 3 hours. Data represent mean and SEM of 3 independent experiments.

Figure 2. Optical density measurements of exponentially growing *E. coli* ATCC 25922 over 5 hours. Data presents mean of 3 independent experiments based. Bacterial growth at 37°C in a 96-well plates from a starting inoculum of OD₆₀₀ of 0.1 has been measured with 8 minutes intervals. (A) Bacteria exposed to antibiotics at MIC concentrations, Ampicillin (4 µg/ml), Tobramycin (0.78 µg/ml), Tetracycline (1 µg/ml) and Ciprofloxacin (0.05 µg/ml). (B) Bacteria exposed to GN-2 peptide at 1x MIC (6.2 µg/ml) and 2x MIC (12.5 µg/ml) and GN-6 peptide at 1x MIC (12.5 µg/ml) and 2x MIC (25 µg/ml) concentrations.

Figure 3. Peptide effect on *E. coli* morphology. (A,B) Flow cytometry data of GN-2 and GN-6 peptide influence on the DNA content per cell mass represented by fluorescence/lightscatter ratio, respectively. Data collected over a course of 3 hours in a microtiter plate format with an inoculum of OD₆₀₀ of 0.1 and incubated at 37°C between extractions. (C) Microscope images of ethanol stained flow cytometry samples of *E. coli* treated with GN-2 and GN-6 peptide at 1x and 4xMIC concentration for 3 hours. Bacteria without cellular content appear transparent. Pictures taken at same magnification with a Leica DM5000 B microscope.

Figure 4. Visualization and quantification of membrane permeabilization of GN-2 peptide on *E. coli* ATCC 25922 over a period of 120 minutes. (A) Control cells. (B) Bacteria exposed to 1xMIC GN-2 peptide. (C) Bacteria exposed to 4xMIC GN-2 peptide. (D) Percentage of live bacteria after treatment with 1x, 2x and 4xMIC concentration of peptide GN-2. Pictures taken with Leica DM5000B microscope using mercury lamp.

Figure 5. Calcein release from POPG:POPC vesicles. (A) Calcein leakage measurements from 20 µM POPG:POPC (7:3) vesicles at 37°C at various peptide concentrations in a 96-well format assay at 60 min. All readings are baseline corrected by subtracting values from wells containing only liposomes. 100% leakage is estimated as a total calcein release from liposomes exposed to 10 % Triton X-100. Represented results are mean values of three independent experiments with good reproducibility. Standard error bars are omitted for clarity. Calcein leakage measurements from 20

μM POPG:POPC (7:3) vesicles at 37°C at various concentrations of **(B)** GN-2, **(C)** GN-6 and **(D)** GN-14, in a 96-well format assay over a period of 1 hour.